Progress In Electromagnetics Research Letters, Vol. 53, 127–135, 2015

Compact Differential Bandpass Filters Based on Coupled-Line Resonators with Improved Performance and Miniaturized Size

Hui Wang*, Yi Yang, Zhi-Hong Ren, and Cheng Feng

Abstract—Two compact differential bandpass filters (BPFs) based on coupled-line resonators and loaded capacitors are proposed in this work. By properly designing the coupled resonator and the loaded capacitance of original filter model, differential-mode (DM) passband responses and common-mode (CM) rejection can be obtained. For validation, two differential BPFs named Filter I and Filter II are discussed and experimentally characterized. One more DM transmission zero generated by out-of-phase cross-coupling is employed to control the DM bandwidth and sharpen the selectivity in Filter I while lumped capacitors are loaded in Filter II to replace capacitive coupled resonators for miniaturized size. Both filters are centered at 4.5 GHz with about 9% DM fractional bandwidth (FBW), less than 1.5 dB insertion loss, more than 15 dB return loss, and wideband CM suppression with more than 18 dB rejection. Furthermore, the size of Filter II is substantially smaller than Filter I and previously reported differential BPFs.

1. INTRODUCTION

Differential bandpass filters (BPFs) with the advantages of higher immunity to the environmental noises, better dynamic range, and lower electromagnetic interference (EMI) [1, 2] are attractive compared with traditional single-ended BPFs. Differential BPFs using 180° phase shift structure were presented in [3] and [4] while microstrip-line resonators were employed in [5–7] with common-mode (CM) suppression. In [8], differential BPF using two broadband planar March and baluns was proposed, and compact wideband differential BPF based on half-wavelength ring resonator was presented in [9]. Ref. [10] focused on theory and application of complementary split-ring resonators (CSRRs) while combining open split ring resonators (OSRRs) and open complementary split ring resonators (OCSRRs) were implemented in [11] for differential BPFs design. In [12], double-sided parallel-strip line and transversal signal-interaction concepts were introduced to achieve differential-mode (DM) filtering and CM rejection. Simple T-shaped resonator was demonstrated in [13] for good differential performances. However, few studies have described the DM selectivity improving as well as size miniaturization.

To realize improved DM selectivity and miniaturized size, compact differential BPFs based on coupled-line resonators and loaded capacitors are proposed in this work. The DM and CM equivalent half circuits of original model are presented and discussed. Two BPFs named Filter I and Filter II are demonstrated on RO4003 with $\varepsilon_r = 3.38$ and $h = 0.508$ mm for validation. Ansoft HFSS is employed for simulation meanwhile the measurement is done by the Anritsu MS4624D vector network analyzer. Their experimental characterizations are in good agreement with theoretical analysis with less than 1.5 dB insertion loss, more than 15 dB return loss, and wideband CM suppression with more than 18 dB rejection. Sharpened skirts and easily controlled bandwidth are exhibited both in Filter I and Filter II. In addition, more than 70% size is miniaturized by loading lumped capacitors in Filter II comparing with Filter I and some previously reported differential BPFs.

Received 3 March 2015, Accepted 21 May 2015, Scheduled 19 June 2015
* Corresponding author: Hui Wang (w_h5300@sina.com).
The authors are with the 28th Research Institute of China Electronics Technology Group Corporation, Nanjing 210007, China.

2. ANALYSIS OF ORIGINAL MODEL

Figure 1(a) shows the equivalent circuit of the original model based on coupled-line resonator. When the DM signals are excited from ports 1 and 1′, a virtual electric wall appears along the symmetric line S-S' and half of part B will be short-ended parallel coupled lines which can be calculated as symmetrical inductive π-network, as shown in Figure 1(b). Similarly, a virtual magnetic wall will appear and half of part B becomes to be a pair of open-ended coupled lines which can be analyzed as capacitive T-network when CM operation is considered in Figure 1(c). The equivalent LC circuit models of DM and CM are presented in Figure 1(d) and Figure 1(e), respectively. And the values of equivalent inductance and capacitance can be calculated as [17]

$$L_1 = -\left[\left(Y_{oo} - Y_{oe}\right)\cot\theta_2\right]/2 \tag{1}$$

$$L_2 = -Y_{oe}\cot\theta_2 \tag{2}$$

$$C_1 = -Z_{oo}\cot\theta_2 \tag{3}$$

$$C_2 = -\left[\left(Z_{oe} - Z_{oo}\right)\cot\theta_2\right]/2 \tag{4}$$

Thus, bandpass responses for DM and wideband rejection for CM can be obtained, as demonstrated in Figure 2 [14, 15]. Although good CM attenuation with more than 20 dB suppression and better than 20 dB DM matching can be found, the DM filtering responses, especially for the controllable bandwidth and selectivity are not good enough for modern wireless systems.

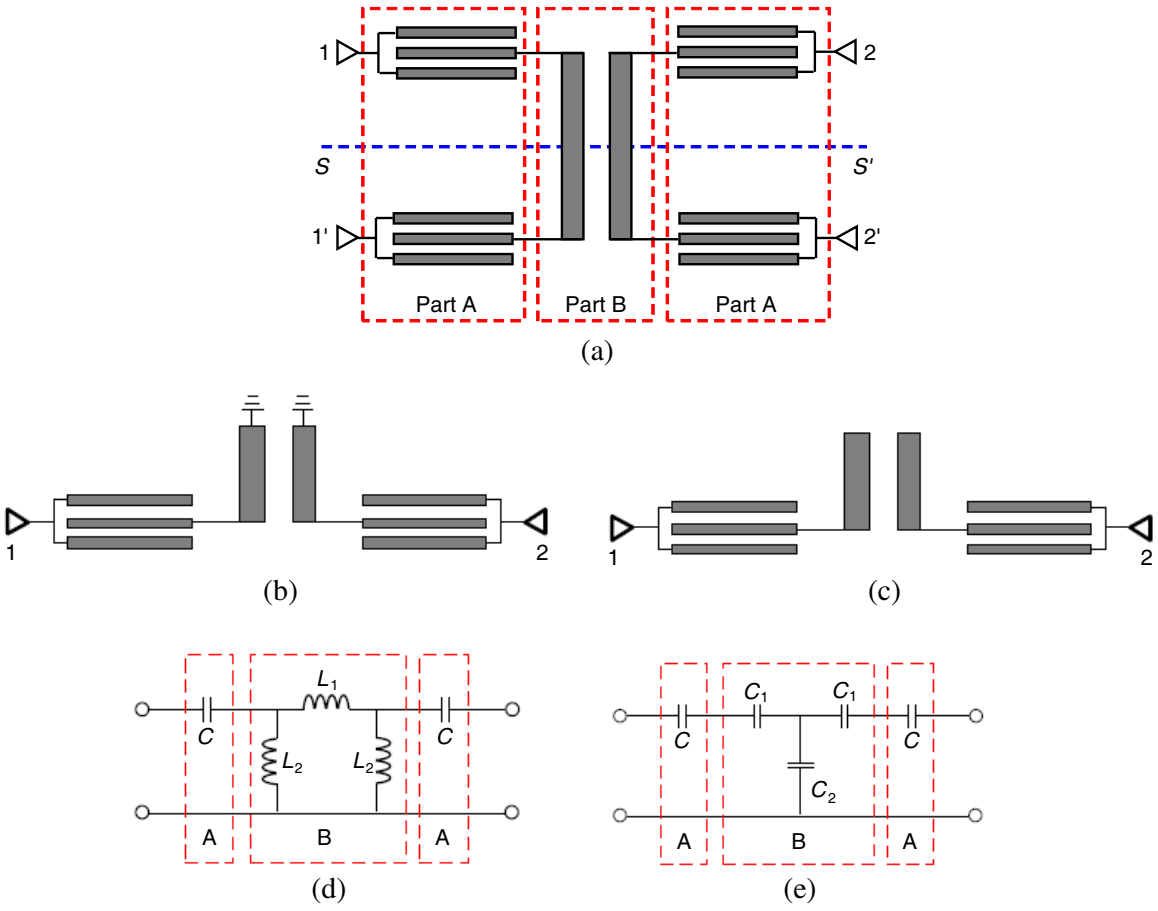

Figure 1. Equivalent circuits of (a) original model, (b) DM, (c) CM, and equivalent LC circuit models of (d) DM, (e) CM.

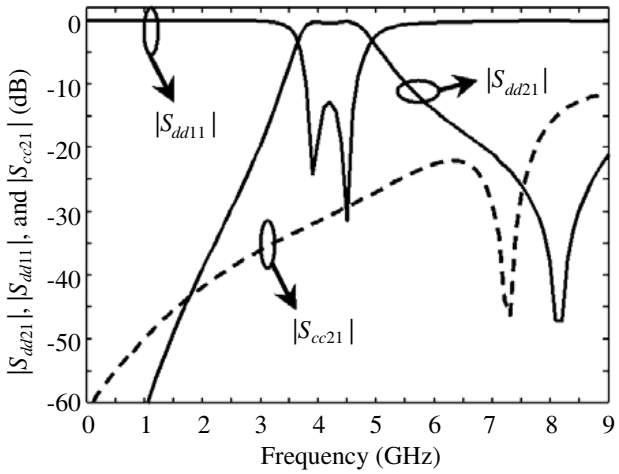

Figure 2. Simulated DM and CM results of the original model.

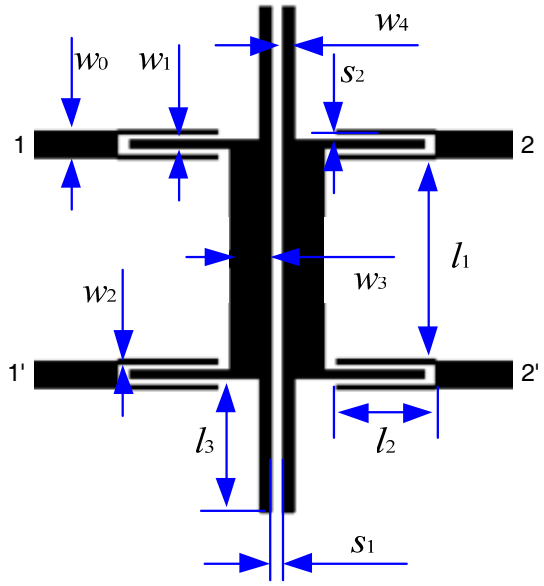

Figure 3. Layout of Filter I.

3. FILTER I WITH IMPROVED DM SELECTIVITY AND CONTROLLABLE BANDWIDTH

To sharpen filter skirt, out-of-phase cross-coupling technique can be employed in Filter I to create one more controllable transmission zero, as plotted in Figure 3. Figure 4(a) illustrates the equivalent circuit of DM circuit in which open-circuited coupled-line resonators loaded. As discussed, the short-circuited coupled lines provide equivalent inductive circuit while open-circuited ones are equivalent capacitive circuit. A coupling diagram is drawn in Figure 4(b), where each node represents a transmission line resonator in Figure 4(a) and M_{ij} denotes coupling between them, the solid lines indicate the main path couplings and the dash line denotes the cross coupling. It is essential that the cross coupling M_{12} is electric coupling and the coupling M_{34} is magnetic coupling, thus the sign of M_{12} is opposite to that of M_{34} and signals in these coupling paths are out of phase. Therefore, the electric and magnetic couplings cancel out each other at some frequency f_z and thus the selectivity of passband can be controlled by adjusting the coupling coefficient M_{12}.

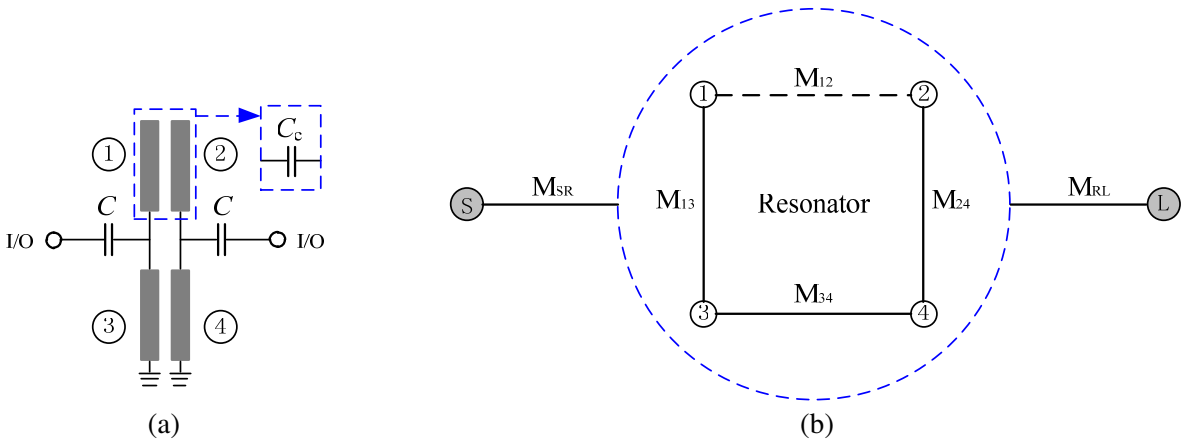

Figure 4. (a) Out-of-phase cross-coupling circuit and (b) general coupling diagram of DM.

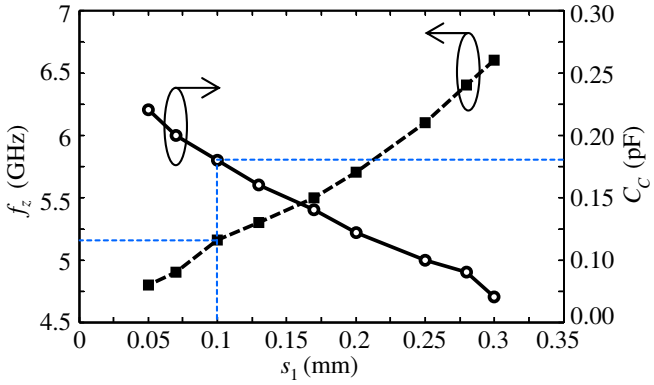

Figure 5. Zero frequency f_z and equivalent capacitance of resonators 1 and 2 versus different gap width s_1.

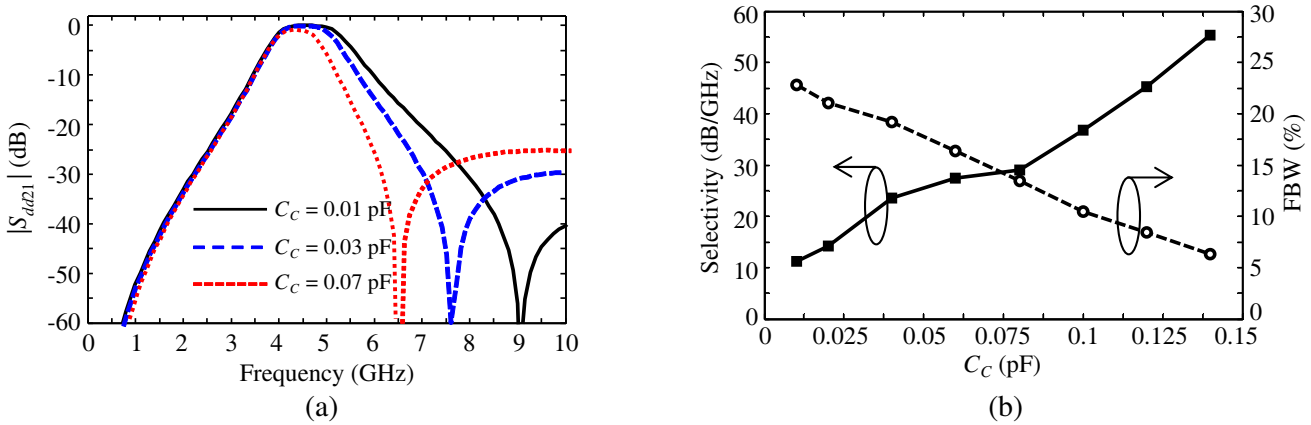

Figure 6. (a) Transmission zero f_z and (b) upper selectivity and FBW of DM responses versus different coupled capacitance C_C.

In addition, the transmission zero f_z and equivalent capacitance C_c of open circuited coupled resonators as shown in Figure 4(a) versus gap width s_1 are presented in Figure 5. It is noted in Figure 5 that C_c is about 0.18 pF and f_z located at 5.2 GHz when $s_1 = 0.1$ mm and $l_3 = 5.6$ mm. Obviously, the fractional bandwidth (FBW) and the upper skirt of DM responses will be affected as the zero f_z moves with different coupled capacitance C_C. In Figure 6(a), the transmission zero decreases from 9.2 GHz to 6.5 GHz for larger C_C. Figure 6(b) plots upper selectivity and FBW versus different C_C, in which the upper selectivity is improved from 11 dB/GHz to 56 dB/GHz while the FBW decreases from 24% to 7% for larger C_C.

For validation, compact differential BPF, i.e., Filter I based on coupled-line resonator is fabricated with $l_1 = 9.4$ mm, $l_2 = 5.0$ mm, $l_3 = 5.6$ mm, $w_0 = 1.17$ mm, $w_1 = 0.4$ mm, $w_2 = 0.2$ mm, $w_3 = 1.2$ mm, $w_4 = 0.15$ mm, and $s_1 = s_2 = 0.1$ mm. The simulated and measured results are illustrated in Figure 7. For DM, the minimum insertion loss is 0.8 dB while the return loss is over 20 dB from 4.3–4.7 GHz with a FBW of 8.9%. The improved sharp upper skirt is obtained with a zero located at $f_z = 5.5$ GHz. For CM, wide suppression range with more than 20 dB attenuation is obtained from *dc* to 8.2 GHz. The filter size is as compact as 22×13.5 mm^2 ($0.18\lambda_0^2$ where λ_0 is the wavelength of 50 Ω microstrip at f_0) as shown in Figure 7(c) although open-circuited coupled resonators are located. The simulated and measured results are in good agreement, confirming our design and discussion.

4. FILTER II WITH MINIATURIZED SIZE

Although less than 0.8 dB DM insertion loss, more than 20 dB DM return loss, improved DM selectivity, controllable bandwidth, and more than 20 dB CM wideband rejection are obtained and depicted in Figure 7, the electric size of Filter I is larger than the original model due to the loaded open-circuited coupled-line resonator.

To miniaturize the size, another differential BPF named Filter II is proposed and discussed.

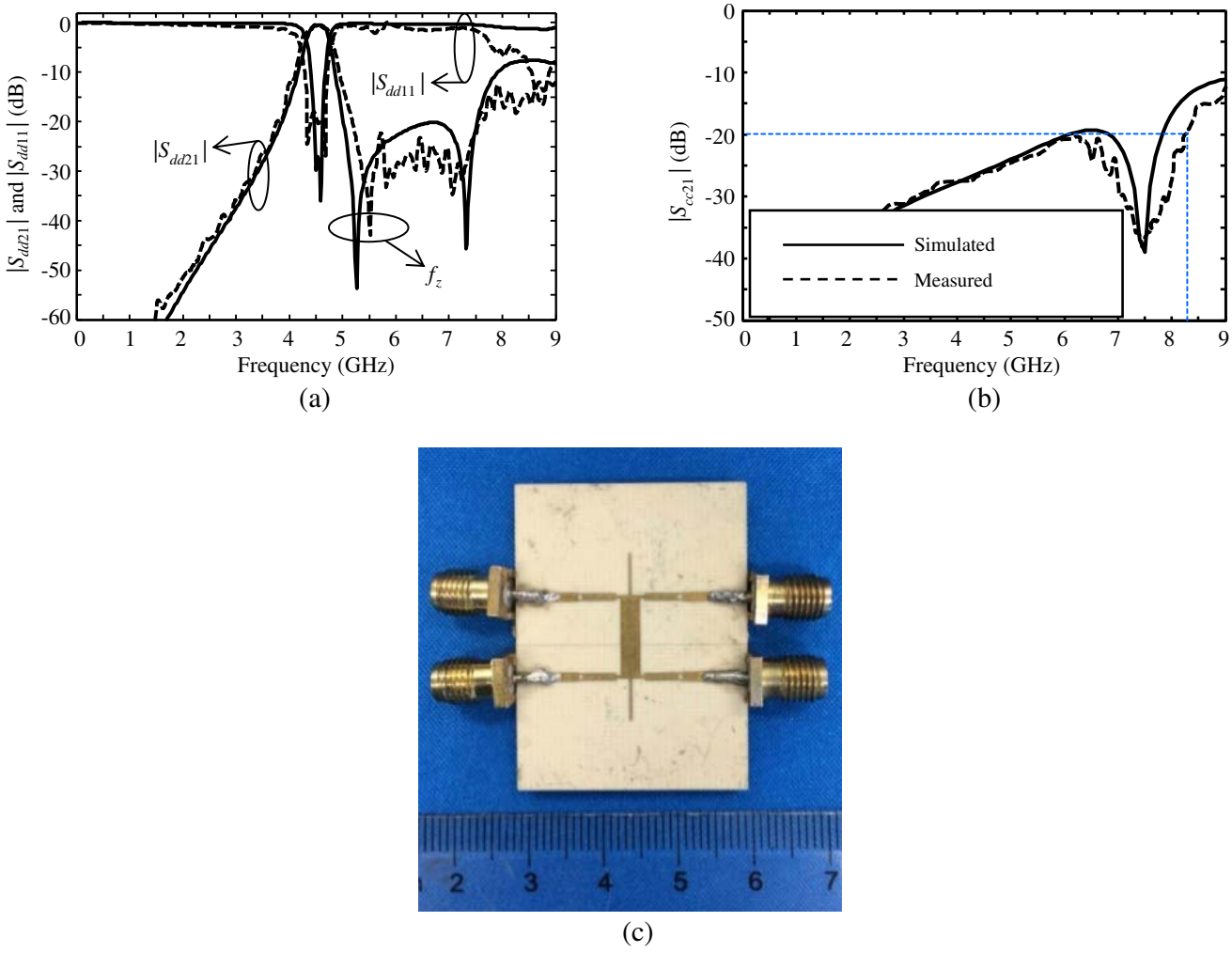

Figure 7. Simulated and measured results of (a) DM insertion loss and return loss and (b) CM rejection and (c) photograph of the proposed differential Filter I.

Table 1. Comparisons of measured results with other differential BPFs.

	Ref. [3]	Ref. [4]	Ref. [8]	Ref. [9]	Ref. [12]	Filter I	Filter II
$\|S_{dd21}\|$ (dB)	−1.19	−1	−1.75	−0.7	−1.6	−0.8	−1.5
$\|S_{dd11}\|$ (dB)	−15	−15	unknown	−10	−15	−20	−15
$\|S_{cc21}\|$ (dB)	−20	−10	−13	−13	−15	−20	−18
Size (λ_0^2)	0.71	1.76	0.29	0.67	0.39	0.18	0.05

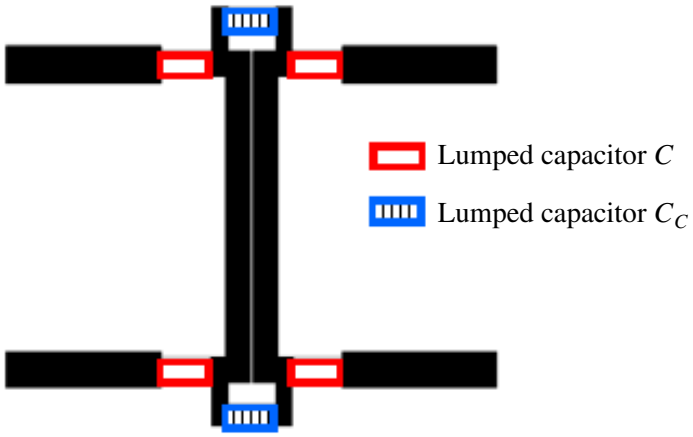

Figure 8. Layout of Filter II.

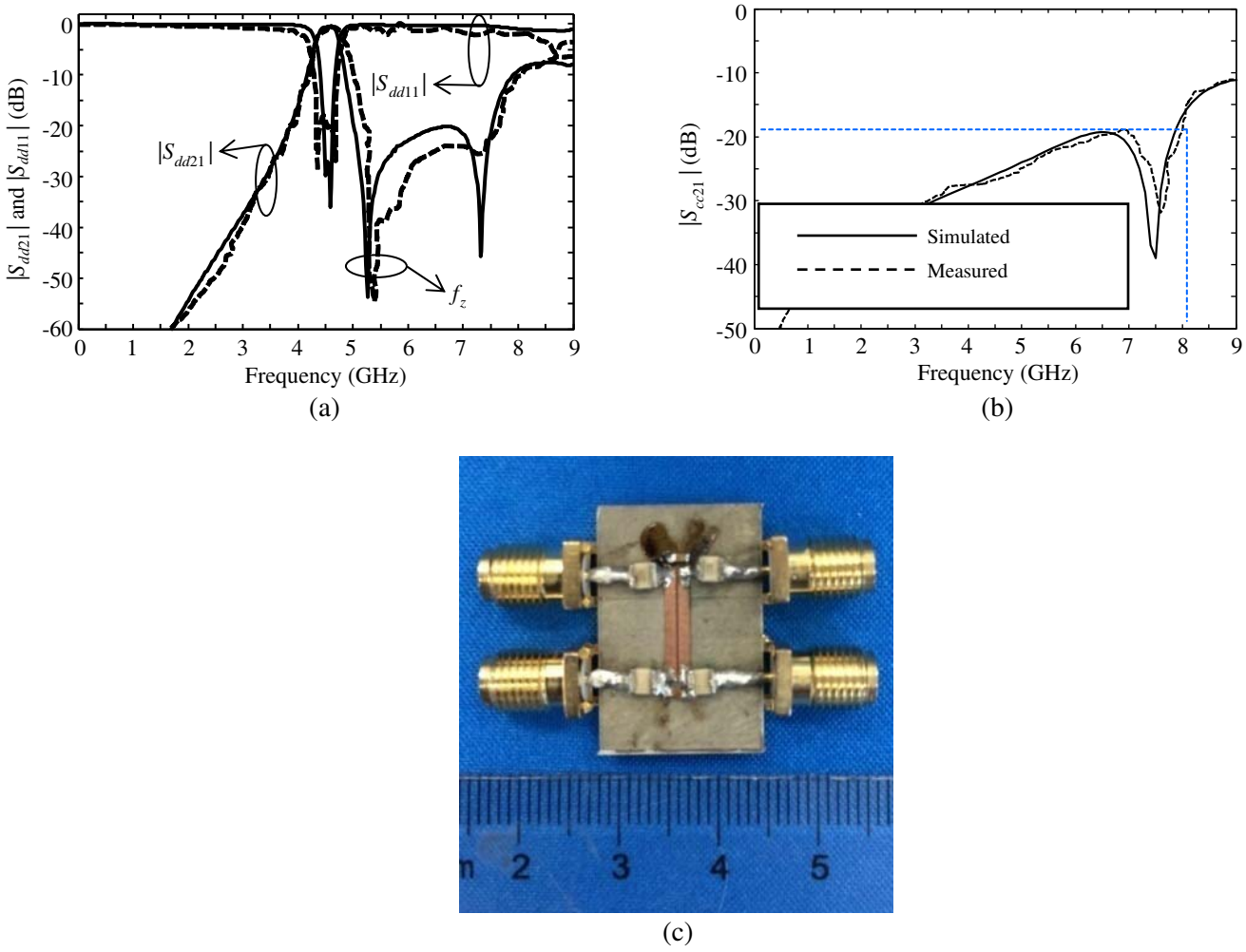

Figure 9. Simulated and measured results of (a) DM insertion loss and return loss and (b) CM rejection and (c) photograph of the Filter II with miniaturized size.

As demonstrated in Figure 8, lumped capacitors, i.e., C and C_C are employed in Filter II to take place of interdigital coupling lines and open-circuited coupled-line resonators, respectively. All the capacitors employed in this work are *DLI C17AH* series high-Q capacitors [16]. The values of equivalent capacitances C and C_C can be calculated as [17–19]

$$C = \frac{10^{-3}\varepsilon_{eff}}{6\pi} R l_2 \tag{5}$$

$$R = \begin{cases} \dfrac{1}{\pi}\ln\left(2\dfrac{1+\sqrt{k}}{1-\sqrt{k}}\right) & 0.707 \le k \le 1 \\ \dfrac{\pi}{\ln\left(2\dfrac{1+\sqrt{k'}}{1-\sqrt{k'}}\right)} & 0 \le k \le 0.707 \end{cases} \tag{6}$$

$$\begin{cases} k = \tan^2\left(\dfrac{w_1\pi}{4(w_1+s_2)}\right) \\ k' = \sqrt{1-k^2} \end{cases} \tag{7}$$

$$C_C = \frac{1}{2}C_1 + C_2 \tag{8}$$

where C_1 and C_2 can be obtained by Equations (3) and (4).

The geometric parameters of Filter II are the same as those presented in the previous section for Filter I expect $l_1 = 8.9\,\text{mm}$, $w_3 = 0.8\,\text{mm}$, $C = 0.4\,\text{pF}$, and $C_C = 0.12\,\text{pF}$. Based on the above theoretical analysis and discussion, Filter II is designed, simulated, and fabricated on Rogers 4003. The simulated and measured S-parameters are plotted in Figures 9(a) and (b) with a photograph shown

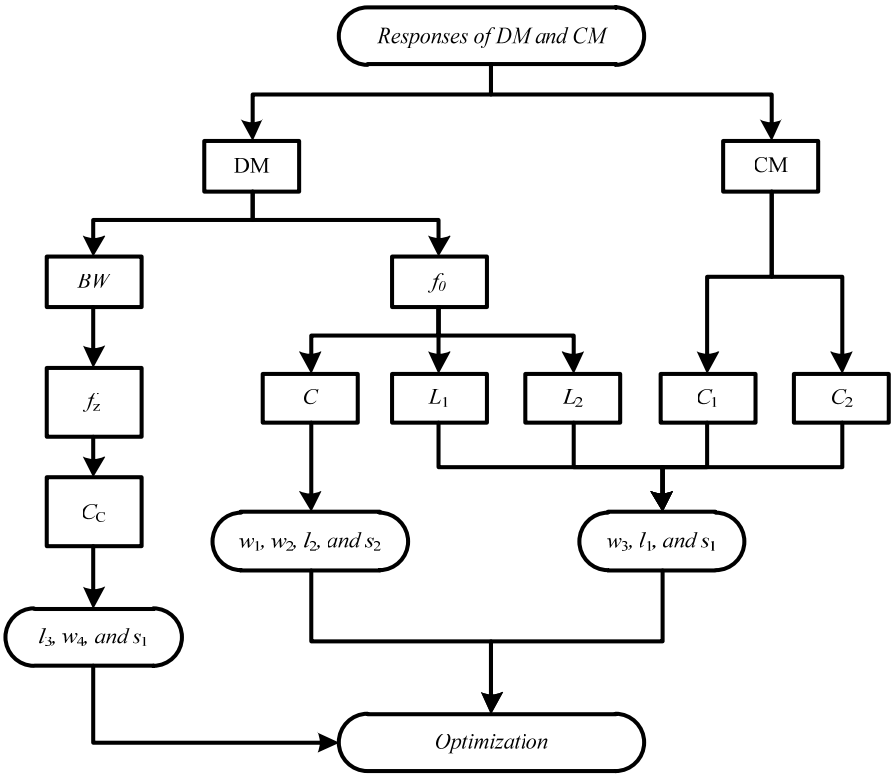

Figure 10. Design procedure of proposed differential filters.

in (c). For DM, the measured insertion loss is less than 1.5 dB while the return loss is over 15 dB from 4.28–4.72 GHz with a 3-dB FBW of 9.7%. For CM, over 18 dB rejection is obtained within 0–8 GHz, indicating very good wideband CM suppression. The total size of the proposed Filter II is only $13.8 \times 5.9\,\text{mm}^2$ ($0.05\lambda^2$). Compared with the Filter I and some previously reported differential BPFs, more than 70% size is reduced. The filter design procedure is summarized as a flow chart in Figure 10.

The measured results of differential BPFs Filter I and Filter II are also compared with some reported differential filters as summarized in Table 1. It is apparent that advantages of differential BPFs presented in this work are demonstrated in DM insertion loss, return loss, and CM suppression. In addition, Filter II based on capacitors loaded shows more than 70% size reduction and not only good DM filtering but also CM suppression compared with Filter I and some previously reported differential BPFs.

5. CONCLUSION

Compact differential BPFs named Filter I and Filter II based on coupled-line resonators are presented and analyzed in this work. One more transmission zero is generated by loading open-circuited coupled lines in Filter I to sharpen the selectivity and realize bandwidth control. For miniaturized size, lumped capacitors are employed in Filter II and more than 70% size is reduced. Very good DM insertion loss, return loss, selectivity, wideband CM suppression, and compact size are exhibited in both Filter I and Filter II. The simulated and measured results are in good agreement indicating that filters discussed in this work are attractive in modern communication systems.

REFERENCES

1. Cai, J. and X. D. Wang, "Electromagnetic compatibility (EMC) test method for vehicle-borne electronic information system," *Command Information System and Technology*, Vol. 5, No. 2, 83–87, Apr. 2014.
2. Hao, J. S. and Y. Wang, "Clutter suppression for ultra-wideband radar," *Command Information System and Technology*, Vol. 4, No. 3, 60–64, Jun. 2013.
3. Wang, X.-H., Q. Xue, and W.-W. Choi, "A novel ultra-wideband differential filter based on double-sided parallel-strip line," *IEEE Microwave and Wireless Components Letters*, Vol. 20, No. 8, 471–473, Aug. 2010.
4. Wang, X.-H., H. Zhang, and B.-Z. Wang, "A novel ultra-wideband differential filter based on microstrip line structures," *IEEE Microwave and Wireless Components Letters*, Vol. 23, No. 3, 128–130, Mar. 2013.
5. Wu, X.-H. and Q.-X. Chu, "Compact differential ultra-wideband bandpass filter with common-mode suppression," *IEEE Microwave and Wireless Components Letters*, Vol. 22, No. 9, 456–458, Sep. 2012.
6. Lim, T.-B. and L. Zhu, "A differential-mode wideband bandpass filter on microstrip line for UWB application," *IEEE Microwave and Wireless Components Letters*, Vol. 19, No. 10, 632–634, Oct. 2009.
7. Lim, T.-B. and L. Zhu, "Highly selective differential-mode wideband bandpass filter for UWB application," *IEEE Microwave and Wireless Components Letters*, Vol. 21, No. 3, 133–135, Mar. 2011.
8. Zhu, H.-T., W.-J. Feng, W.-Q. Che, and Q. Xue, "Ultra-wideband differential bandpass filter based on transversal signal-interference concept," *IET Electronics Letters*, Vol. 47, No. 18, 1033–1035, Sep. 2011.
9. Feng, W.-J., W.-Q. Che, Y.-L. Ma, and Q. Xue, "Compact wideband differential bandpass filters using half-wavelength ring resonator," *IEEE Microwave and Wireless Components Letters*, Vol. 23, No. 2, 81–83, Feb. 2013.
10. Naqui, J., A. Fernandez-Prieto, M. Duran-Sindreu, F. Mesa, J. Martel, F. Medina, and F. Martin, "Common-mode suppression in microstrip differential lines by means of complementary split ring

resonators: Theory and application," *IEEE Transactions on Microwave Theory and Techniques*, Vol. 60, No. 10, 3023–3034, Oct. 2012.

11. Velez, P., J. Naqui, A. Fernandez-Prieto, M. Duran-Sindreu, J. Bonache, J. Martel, F. Medina, and F. Martin, "Differential bandpass filter with common-mode suppression based on open split ring resonators and open complementary split ring resonators," *IEEE Microwave and Wireless Components Letters*, Vol. 23, No. 1, 22–24, Jan. 2013.
12. Feng, W.-J., W.-Q. Che, T.-F. Eibert, and Q. Xue, "Compact wideband differential bandpass filter based on the double-sided parallel-strip line and transversal signal-interaction concepts," *IET Microwave, Antennas & Propagation*, Oct. 2011.
13. Feng, W.-J. and W.-Q. Che, "Novel wideband differential bandpass filters based on T-shaped structure," *IEEE Transactions on Microwave Theory and Techniques*, Vol. 60, No. 6, 1560–1568, Jun. 2012.
14. Wang, H., K.-W. Tam, S.-K. Ho, and W. Wu, "A novel compact capacitive loaded differential bandpass filter," *Asia-Pacific Microwave Conference*, 933–935, Seoul, Korea, 2013.
15. Wang, H., K.-W. Tam, W.-W. Choi, W.-Y. Zhuang, S.-K. Ho, W. Kang, and W. Wu, "Analysis of coupled cross-shaped resonator and its application to differential bandpass filters design," *IEEE Transactions on Microwave Theory and Techniques*, Vol. 62, No. 12, 2942–2953, Dec. 2014.
16. Available: http://www.dilabs.com.
17. Matthaei, G.-L., L. Young, and E.-M.-T. Jones, *Microwave Filters, Impedance-matching Networks, and Coupling Structures*, Artech House, Chapter 5, Norwood, MA, USA, 1985.
18. Alley, G. D., "Interdigital capacitors and their application to lumped-element microwave integrated circuits," *IEEE Transactions on Microwave Theory and Techniques*, Vol. 18, No. 12, 1028–1033, Dec. 1970.
19. Pettenpaul, E., H. Kapust, A. Weisgerber, H. Mampe, J. Luginsland, and I. Wolff, "CAD models of lumped elements on GaAs up to 18 GHz," *IEEE Transactions on Microwave Theory and Techniques*, Vol. 36, No. 2, 294–304, Feb. 1988.